

Hund's rule Magnetism in C_{60} ions?

Martin Lüders^{1,2,3}, Nicola Manini^{1,4,5}, Paolo Gattari⁴, and Erio Tosatti^{1,2,6}

¹ International School for Advanced Studies (SISSA), Via Beirut 4, 34014 Trieste, Italy

² INFN Democritos National Simulation Center, and INFN, Unità Trieste, Italy

³ Daresbury Laboratory, Warrington WA4 4AD, UK

⁴ Dip. Fisica, Università di Milano, Via Celoria 16, 20133 Milano, Italy

⁵ INFN, Unità di Milano, Milano, Italy

⁶ International Centre for Theoretical Physics (ICTP), P.O. Box 586, 34014 Trieste, Italy

Abstract. We investigate the occurrence of Hund's rule magnetism in $C_{60}^{n\pm}$ molecular ions, by computing the ground-state spin for all charge states n from -3 to $+5$. The two competing interactions, electron-vibration (e-v, including Jahn Teller, favoring low spin) and electron-electron (e-e, including Hund-rule exchange, favoring high spin), are accounted for based on previously computed ab-initio coupling parameters. Treating the ion coordinates as classical, we first calculate and classify the static Jahn-Teller distorted states for all n , inclusive of both e-v and e-e effects. We then correct the adiabatic result by including the zero-point energy lowering associated with softening of vibrations at the adiabatic Jahn-Teller minima. Our overall result is that while, like in previous investigations, low-spin states prevail in negative ions, Hund's rule high spin dominates all positive C_{60}^{n+} ions. This suggests also that Hund-rule magnetism could arise in fullerene cation-based solid state compounds, particularly those involving C_{60}^{2+} .

PACS. 36.40.Cg Electronic and magnetic properties of clusters – 61.48.+c Fullerenes and fullerene-related materials (structure) – 71.20.Tx Fullerenes and related materials; intercalation compounds (electronic structure) – 75.75.+a Magnetic properties of nanostructures

1 Introduction

Magnetism without transition metals is a potentially exciting subject. As an example, carbon magnetism has generated some recent interest, in connection with some fullerene-derived carbon-only magnetic materials [1,2]. In these materials however the fullerene cage is disrupted into some sort of three-dimensional bonding network. In this paper we focus on carbon magnetism that may occur in isolated fullerene ions, and in ionic fullerene compounds where electrons are added or subtracted to C_{60} molecules that preserve their overall molecular integrity.

Unconventional properties, including magnetism, of negative C_{60} ions have in fact been previously discussed in the literature. Due to the high symmetry of the molecule, the threefold degenerate t_{1u} molecular orbital of C_{60} will, when partly filled, be affected by Coulomb exchange [3,4,5], which favors molecular Hund's rule magnetism, quite similar to that leading to the atomic magnetic moments in ordinary d and f elements and compounds. In addition to displaying Hund-rule physics, a high-symmetry molecule will however also undergo Jahn-Teller (JT) distortions. The JT ground state favors electron spin pairing, generally leading to larger energy gains for low-spin states than for high-spin states. Molecular Hund-rule exchange and JT are therefore competing effects from the point of view

of magnetism. Past studies indicated that in C_{60}^{n-} ions the JT interaction is in fact somewhat stronger than Coulomb exchange, leading to low-spin ground states [5,6,7,8,9].¹ Nonetheless, the balance between JT and Hund's rule is to some degree compound dependent, leading to a close match in certain chemical environments. Spin gaps of the order of 100 meV between the $S = 0$ ground state and the $S = 1$ excitation of the C_{60}^{2-} or equivalently of the C_{60}^{4-} ion were reported in NMR studies of compounds like K_4C_{60} and Na_2C_{60} , but a narrower 10 meV gap has been suggested for the $n = -2$ fluctuating charge state in CsC_{60} [12]. The magnetism of TDAE- C_{60} [13,14] can also be at-

¹ Low-spin ground state is also observed in a number of diradicals [10,11], but the situation there is quite different from C_{60} ions. In ideal icosahedral C_{60} ions the degenerate orbitals require a regular first Hund rule with maximum spin. Density-functional theory (DFT) calculations do of course confirm that. A low-spin ground state may be eventually obtained if, upon lowering the icosahedral symmetry by means of a JT distortion, the corresponding energy gain happened to be large enough to reverse the undistorted high-spin situation. In the aromatic diradicals instead, two distant unpaired spins interact somewhat weakly through the molecular backbone, and a Heitler-London singlet ground state appears to be achieved, no distortions involved.

tributed to a spin triplet in charge fluctuating C_{60}^{2-} states [15].

The main question which we wish to address here is what ground-state spin is to be expected for positive C_{60}^{n+} ions. The calculations will be done in parallel for C_{60}^{n+} and C_{60}^{n-} so as to emphasize the analogies and the differences that will emerge. Zero-point effects are also approximately included, and their effect is shown to be non negligible.

Data on C_{60}^{n+} molecular ions do not appear to be readily available. In particular the published photoemission spectra of C_{60} [16,17] imply C_{60}^+ final states. This $n = 1$ state is affected by JT but clearly not by Hund's rule. Some charge-transfer compounds contain nominal C_{60}^{2+} ions. While it is presently unclear whether higher charge states are accessible, acceptor compounds with nominal $(AsF_6)_2 C_{60}$ and $(SbF_6)_2 C_{60}$ stoichiometries have been described, containing again C_{60}^{2+} molecular ions. Recent data, including anomalously short spin-lattice relaxation times [18], strongly suggest the possibility of magnetism of the C_{60}^{2+} ions.

Here we address the question of magnetism of C_{60}^{n+} ions by addressing quantitatively the competition between JT and Coulomb exchange in these ions. Both JT and intramolecular exchange terms are calculated to be individually stronger in C_{60}^{n+} than in C_{60}^{n-} [5,19]. Preliminary calculations and estimates based on the adiabatic approximation [5] did foreshadow the predominance of Hund's rule exchange in C_{60}^{n+} , as opposed to the predominance of JT in C_{60}^{n-} . In the adiabatic approximation however, the JT effect is postulated to be static, neglecting zero-point motion of the carbon nuclei (responsible for turning JT from static to dynamic, even at $T = 0$). This simplification might be unsafe, as it is known to underestimate the JT energy gain [8]. In turn, it might seriously impair our understanding of the competition between high spin and low spin, through the neglect of very large corrections associated to the different zero-point vibrational quantum kinetic energy associated with states of different spin. Here we estimate these zero-point effects and include them in the coupled JT-Hund's rule problem, thus correcting the adiabatic result. An accurate evaluation of this correction is in fact quite generally a formidable task. We show here that one lucky feature of C_{60}^{n+} ions is that their strong e-v coupling makes the basic zero-point correction a good approximation to the true result. Our bottom-line conclusion will be that whereas quantum corrections to the ground state energy are confirmed to be large, they do not reverse the ground-state spin state for any of the C_{60}^{n+} ions. In particular the prediction that C_{60}^{2+} should be magnetic is maintained. It is in fact reinforced, with the $S = 1$ ground state about 30 meV lower than the lowest $S = 0$ state.

This prediction does not of course imply that compounds containing C_{60}^{n+} will by necessity be magnetic. Electron kinetic energy associated with hopping between molecules do in principle favor band electron spin pairing, and a standard nonmagnetic metallic state. However, any insulating states that could arise due to very narrow bands, such as a Mott or more probably a Mott-JT

insulator[20], is very likely to be magnetic. In this regard it seems interesting that both $(AsF_6)_2 C_{60}$ and $(SbF_6)_2 C_{60}$ acceptor intercalated materials, nominally containing doubly positive fullerene ions were indeed found to be electrical insulators, with activation gaps of 0.22 and 0.64 eV respectively [21].

The starting point of this paper will be the static, adiabatic JT-distorted state of all $C_{60}^{n\pm}$ ions treated in the simplest model Hamiltonians that includes both e-v and e-e interactions. Each of these static JT wells, or "valleys", is characterized by a reduction of symmetry from icosahedral to some subgroup. New vibrational frequencies arise at each such valley. We determine these frequencies by evaluation of the Hessian energy matrix at the energy minimum [22]. We use the lowering of the zero-point vibrational energies from the undistorted to the JT distorted state to estimate the leading quantum correction to the adiabatic approximation. The next-order quantum correction would arise from weak tunneling between equivalent valleys. This is the conceptually important step that leads from static to dynamic JT, with full restoration of the undistorted icosahedral symmetry. The associated energy correction expected is however relatively minor in C_{60}^{n+} , in view of the large e-v couplings. In the limit of infinite coupling the tunneling corrections vanish, and all quantum effects coincide exactly with the zero-point lowering. Therefore, a direct quantitative check that the tunneling corrections are reasonably small already in the weakest coupling case of C_{60}^{1-} , and already negligible in C_{60}^{1+} justifies us in neglecting them for all other charge states. The accuracy of this neglect is, it should be noted, particularly good for the positive ions C_{60}^{n+} , where the e-v coupling is larger than in C_{60}^{n-} .

This paper is organized as follows. Sect. 2 introduces the model and the parameters used in this calculation, which is then described in Sect. 3, along with the properties of the JT valleys for all values n and S . The zero-point non-adiabatic corrections are described in Sect. 4, and the overall results are finally discussed in Sect. 5.

2 The model Hamiltonian

We begin by reviewing here the model Hamiltonian previously introduced in Ref. [5] to describe the electron-vibration coupling and Coulomb exchange of holes in the h_u fivefold-degenerate highest occupied molecular orbital (HOMO), and of electrons in the threefold-degenerate t_{1u} lowest unoccupied molecular orbital (LUMO) of C_{60} :

$$\hat{H} = \hat{H}_0 + \hat{T}_{\text{vib}} + \hat{V}_{\text{vib}} + \hat{H}_{e-v} + \hat{H}_{e-e} \quad (1)$$

where

$$\hat{H}_0 = \epsilon \sum_{\sigma m} \hat{c}_{\sigma m}^\dagger \hat{c}_{\sigma m}, \quad (2)$$

$$\hat{T}_{\text{vib}} = \sum_{i\Lambda\mu} \frac{\hbar\omega_{i\Lambda}}{2} \hat{P}_{i\Lambda\mu}^2, \quad (3)$$

$$\hat{V}_{\text{vib}} = \sum_{i\Lambda\mu} \frac{\hbar\omega_{i\Lambda}}{2} \hat{Q}_{i\Lambda\mu}^2 \quad (4)$$

$$\hat{H}_{e-v} = \sum_{r i\Lambda} \frac{k^A g_{i\Lambda}^r \hbar\omega_{i\Lambda}}{2} \sum_{\sigma m m' \mu} C_{m m'}^{r A \mu} \hat{Q}_{i\Lambda\mu} \hat{c}_{\sigma m}^\dagger \hat{c}_{\sigma -m'} \quad (5)$$

$$\hat{H}_{e-e} = \frac{1}{2} \sum_{\sigma, \sigma'} \sum_{\substack{m m' \\ k k'}} w_{\sigma, \sigma'}(m, m'; k, k') \hat{c}_{\sigma m}^\dagger \hat{c}_{\sigma' m'}^\dagger \hat{c}_{\sigma' k'} \hat{c}_{\sigma k} \quad (6)$$

are respectively the one-electron Hamiltonian, the vibron kinetic energy, the harmonic restoring potential toward the equilibrium configuration of neutral C₆₀, the electron-vibron coupling (in the linear JT approximation) [19, 23], and finally the mutual Coulomb matrix element representing intra-molecular repulsion between the holes/electrons [5]. Here $\hat{c}_{\sigma m}^\dagger$ denote creation operators of either a hole in the HOMO or an electron in the LUMO, described by the single-particle wave functions $\varphi_{m\sigma}(\mathbf{r})$. σ indicates the spin projection; m labels the component within the degenerate electronic multiplets, according to the C_5 character from the $I_h \supset D_5 \supset C_5$ group chain [23, 24]. i enumerates the vibration modes of symmetry Λ (2 A_g , 8 H_h , and 6 G_g modes, the latter being JT active in the hole case only). $C_{m m'}^{r A \mu}$ are Clebsch-Gordan coefficients [24] of the icosahedral group I_h , for coupling h_u/t_{1u} states to phonons of symmetry Λ . r is a multiplicity label, relevant for h_u holes and H_g vibrations only, where it takes two values, 1 and 2 [19, 24]. $\hat{Q}_{i\Lambda\mu}$ are the dimensionless molecular normal-mode vibration coordinates (measured from the adiabatic equilibrium configuration of neutral C₆₀, in units of the length scale $x_0(\omega_{i\Lambda}) = \sqrt{\hbar/(\omega_{i\Lambda} m_C)}$ associated with each harmonic oscillator where m_C is the mass of the C atom), and $\hat{P}_{i\Lambda\mu}$ the corresponding conjugate momenta. Finally, spin-orbit, exceedingly small in C₆₀ [25], is neglected throughout.

For holes, the JT model defined by Eq. (3), (4), (5), for C₆₀ⁿ⁺ is conventionally denoted as $h^n \otimes (A + G + H)$: h^n refers to the hole occupancy of the h_u HOMO, and A , G , H refer to the 2 nondegenerate A_g , 6 fourfold-degenerate G_g and 8 fivefold-degenerate H_g molecular vibration modes that are linearly coupled to h_u in icosahedral symmetry [19, 23, 26]. For electrons, the JT model is $t^n \otimes (A + H)$, t^n referring to n electrons occupying the t_{1u} LUMO, linearly coupled to the 2 A_g and 8 H_g vibrational modes only. In all calculations we shall adopt the numerical values of the e-v coupling parameters $g_{i\Lambda}^r$, listed in Table 1, previously obtained from first-principles Density DFT electronic structure calculations in Ref. [19]. A recent DFT calculation [27] based on a different functional reported couplings that are similar on the whole to those of Table 1, the main difference concerning a closer competition between D_{3h} and D_{5d} valleys for the distortion of C₆₀¹⁻. The JT stabilization energy based on the DFT parameters of Ref. [19] is only about one fifth of that found based on the intermediate neglect of differential overlap (INDO) model [28]. We think that these earlier calculations, as well as more recent Hartree-Fock (HF) estimates [29] also suggesting large e-v couplings and energy gains are somewhat less dependable. We believe the

Table 1. Computed vibrational eigenfrequencies, and e-v linear coupling parameters for the h_u HOMO and t_{1u} LUMO in C₆₀ [19].

	$\hbar\omega_{i\Lambda}$ cm ⁻¹	$\hbar\omega_{i\Lambda}$ meV	$g_{i\Lambda}^1$ (HOMO)	$g_{i\Lambda}^2$ (HOMO)	$g_{i\Lambda}$ (LUMO)
A_g	500	62.0	0.0591	-	0.1565
	1511	187.4	0.2741	-	0.3403
G_g	483	59.9	0.7567	-	-
	567	70.3	0.1024	-	-
	772	95.7	0.8003	-	-
	1111	137.8	0.6239	-	-
	1322	163.9	0.2277	-	-
	1519	188.4	0.4674	-	-
H_g	261	32.4	3.0417	-0.0045	0.4117
	429	53.2	1.0587	0.6131	0.4886
	718	89.0	0.0103	0.9950	0.3500
	785	97.3	0.7836	-0.0309	0.2238
	1119	138.7	0.0514	0.2151	0.1930
	1275	158.0	0.4586	0.2440	0.1382
	1456	180.5	0.8482	0.4530	0.3152
	1588	196.9	0.7436	-0.4488	0.2893

Table 2. The Coulomb parameters for C₆₀^{n±}, defining \hat{H}_{e-e} through (6) and (7), as obtained from the DFT calculations of Ref. [5].

	Parameter	Value [meV]
HOMO (C ₆₀ ⁿ⁺)	F_1	15646
	F_2	105
	F_3	155
	F_4	47
	F_5	0
	U	3097
LUMO (C ₆₀ ⁿ⁻)	J	32
	U	3069

smaller DFT JT gains more realistic for two main reasons: (i) the HF calculations miss an important loss of correlation energy due to opening of the JT gap; (ii) preliminary results indicate that the HOMO photoemission spectrum based on the DFT parameters [30] is in very good agreement with experiment [16, 17]. By contrast, for C₆₀⁻, DFT computed electron-phonon couplings [31, 32, 33, 34] appear to be significantly smaller than those obtained from photoemission of C₆₀⁻ [35]. While we can offer no explanation for that discrepancy in negative ions, we note that the DFT-derived couplings used here for C₆₀ⁿ⁺ are probably also slightly underestimated, however probably only by some 10 to 20%.

The e-v couplings $g_{i\Lambda}^r$ in Eq. (5) are dimensionless, measured in the units of the corresponding harmonic vi-

brational energy quantum $\hbar\omega_{i\Lambda}$. Modes (e.g. the second G_g mode) with $g_{i\Lambda}^r \ll 1$ are thus only weakly coupled; conversely, modes (e.g. the lowest H_g mode) with a large $g_{i\Lambda}^r > 1$ are strongly e-v coupled. The numerical factors $k^{A_g} = 5^{\frac{1}{2}}$, $k^{G_g} = (5/4)^{\frac{1}{2}}$, $k^{H_g} = 1$ for the HOMO, and $k^{A_g} = 3^{\frac{1}{2}}$, $k^{H_g} = 6^{\frac{1}{2}}$ for the LUMO are introduced for compatibility with the normalization of the e-v parameters in Ref. [19].

The Coulomb matrix elements are defined by:

$$w_{\sigma,\sigma'}(m, m'; k, k') = \int d^3r \int d^3r' \quad (7)$$

$$\varphi_{m\sigma}^*(\mathbf{r}) \varphi_{m'\sigma'}^*(\mathbf{r}') u_{\sigma,\sigma'}(\mathbf{r}, \mathbf{r}') \varphi_{k\sigma}(\mathbf{r}) \varphi_{k'\sigma'}(\mathbf{r}')$$

where $u_{\sigma,\sigma'}(\mathbf{r}, \mathbf{r}')$ is an effective Coulomb repulsion, screened by all other electrons of the molecule (eventually also by electrons in all other molecules in a solid state compound; but we shall focus here on the isolated ion). A detailed symmetry analysis [5] shows that, assuming spin-independence of the orbitals, this set of coefficients can be expressed as

$$w_{\sigma,\sigma'}(m, m'; k, k') = \sum_{r,r',\Lambda} F^{r,r',\Lambda} \left(\sum_{\mu} C_{mk}^{r\Lambda\mu} C_{m'k'}^{r'\Lambda\mu} \right) \quad (8)$$

in terms of a minimal set of independent Slater-type parameters $F^{r,r',\Lambda}$ [36]. A DFT estimate of these parameters was previously obtained in Ref. [5], and for our calculation we adopt those values of the Coulomb parameters. They are reproduced for completeness in Table 2. Other sets of couplings, obtained by means of a simple (and clever) model for the HOMO and LUMO orbitals [37] and by a fit to multi-configuration HF calculations [29], are in substantial agreement with each other, but they are both much larger than the DFT couplings of Ref. [5], due to complete neglect of screening. We believe that the actual Coulomb parameters of C_{60} lie somewhere in between the DFT couplings used here and the ‘‘bare’’ ones of Ref. [37, 29], but most likely closer to the DFT ones, due to the large polarizability of C_{60} .

For the HOMO Coulomb parameters we use the short-hands

$$F_1 = F^{A_g}, \quad F_2 = F^{G_g}, \quad F_3 = F^{1,1,H_g}, \quad (9)$$

$$F_4 = F^{2,2,H_g}, \quad F_5 = F^{1,2,H_g}.$$

The Coulomb energy connected with the total molecular charge fluctuation in the HOMO, conventionally called the hole ‘‘Hubbard U’’ is given by the combination

$$U = \left(\frac{F_1}{5} - \frac{4F_2}{45} - \frac{F_3}{9} - \frac{F_4}{9} \right). \quad (10)$$

For electrons in the LUMO, we have instead an electron Hubbard U given by $U = F^{A_g}/3 - F^{H_g}/3$ and a Hund-rule exchange $J = F^{H_g}/2$.

In either case, of electron or of holes, U defines an average Coulomb repulsion within the multiplet of states

of that molecular ion $C_{60}^{n\pm}$, such that the average energy for each n

$$E^{\text{ave}}(n) = \epsilon n + U \frac{n(n-1)}{2}. \quad (11)$$

We observe that U differs from a more common definition of the Hubbard repulsion in lattice models, which involves the lowest state in each n -configuration: $U^{\text{min}} = E^{\text{min}}(n+1) + E^{\text{min}}(n-1) - 2E^{\text{min}}(n)$. This second definition is inconvenient here, since it depends wildly on n . The Hubbard U's are given here for completeness, and because they will be useful in different contexts. However we must recall that the U term is irrelevant for the determination of the ground-state spin of each $C_{60}^{n\pm}$ ion.

3 The adiabatic JT valleys

Though a rather idealized description of real $C_{60}^{n\pm}$ ions, the model Hamiltonian (1), does nevertheless not lend itself to an exact solution. The vibronic eigenstates are generally complicated combinations in the direct product of each (up to 252-dimensional) fixed- n electronic space, times the infinite-dimensional space of the vibrational degrees of freedom. Even with the help of spin and orbital symmetries, exact solutions of the quantum problem (1) are only available in two limiting cases, namely the limit of weak e-v coupling [8, 38, 39] and that of infinitely strong e-v coupling [7, 22, 26, 40]. For $C_{60}^{n\pm}$, where the couplings range from intermediate to large, some approximations are therefore called for. If the phonon kinetic term \hat{T}_{vib} is neglected in the so-called adiabatic approximation, the distortion operators $\hat{Q}_{i\Lambda\mu}$ are replaced by c-number coordinates. This approximation yields the leading ground-state energy lowering $\propto \sum (g_{i\Lambda}^r)^2 \hbar\omega_{i\Lambda}$, exact in the limit of large e-v couplings $g_{i\Lambda}^r \rightarrow \infty$. [Note however that, in this limit, both initial assumptions of harmonic vibrations (4) and of linear e-v coupling (5) become anyway questionable]. In Sect. 4 we shall deal with the leading quantum corrections to the adiabatic approximation $\propto \sum (g_{i\Lambda}^r)^0 \hbar\omega_{i\Lambda}$ by taking zero-point energy shifts into account.

The classical treatment of the vibration coordinates breaks the full molecular symmetry (here icosahedral symmetry) in all configurations possessing a nonzero distortion $Q_{i\Lambda\mu}$ ($\Lambda = G_g, H_g$). Therefore states of different icosahedral symmetry representations are in general intermixed, leaving only the total number of holes n , the total spin S and its projection S_z conserved in the adiabatic ground state. Here we will assume the orbitals to remain basically unchanged upon JT distortion, thus neglecting any small JT-induced change of the Coulomb Hamiltonian \hat{H}_{e-e} . The latter is therefore still determined according to Eqs. (6,7,8) by the same parameters F_i of Table 2, as in the undistorted icosahedral configuration. We will also assume no change of the vibration frequencies $\omega_{i\Lambda}$ and couplings $g_{i\Lambda}^r$ upon charging. While this is of course at variance with much established evidence showing vibration frequency shifts in the percent range per each added electron, it is perfectly in line with the other approximations intrinsic in our model, and in its solution. We leave the

A_g modes out of the adiabatic calculation, since despite their nonzero linear e-v coupling they simply contribute a trivial spin- and symmetry-independent term

$$E^{A_g}(n) = -\frac{1}{8}n^2 \sum_i g_{iA_g}^2 \hbar\omega_{iA_g} = -an^2; \quad (12)$$

$$a = 1.79 \text{ meV (HOMO)}, \quad a = 2.90 \text{ meV (LUMO)},$$

to the total energy $E^{\text{ave}}(n)$ [Eq. (11)], which could effectively be included into U . Because of particle-hole symmetry (exchanging creation and annihilation operators) of the Hamiltonian (excluding H_0 , the A_g modes and the average U contribution), positive charges $n > 5$ can always be mapped onto $n \leq 5$, and negative $n > 3$ onto $n \leq 3$.

For each charge n and spin S and as a function of the vibration coordinates \mathbf{Q} , the lowest adiabatic potential surface $V_{n,S}^{\text{ad}}(\mathbf{Q})$ is obtained as the sum of the lowest eigenvalue of $\hat{H}_{e-e} + \hat{H}_{e-v}(\mathbf{Q})$ in the n -electron spin- S sector, plus the harmonic restoring term $V_{\text{vib}}(\mathbf{Q})$. Allowing the 64 ($6 \times 4 G_g$ ² plus $8 \times 5 H_g$.) vibration coordinates \mathbf{Q} to relax, we determine the optimal distortions \mathbf{Q}_{min} by full minimization of $V_{n,S}^{\text{ad}}(\mathbf{Q})$ in the space of all vibration coordinates \mathbf{Q} . Details of this minimization were previously reported in Ref. [5,41].

Table 3 summarizes the optimal adiabatic energies $E_{\text{adiab}}(n, S) = V_{n,S}^{\text{ad}}(\mathbf{Q}_{\text{min}})$. The separate vibration, e-v, and exchange contributions are specified. The results show that the adiabatic valley minima of positive C₆₀ ions are systematically lower for high-spin states, while the adiabatic outcome for negative ions favors marginally low spin, and is essentially uncertain, with small and poorly reliable energy differences between high- and low-spin states.

Positive and negative ions differ qualitatively also in the geometric nature of the JT distortions characterizing the minimal valleys in the space of coordinates \mathbf{Q} . The $t^n \otimes H$ model applicable to electrons in C₆₀⁻ leads to a flat continuous manifold of equivalent points. The valleys are really troughs, which could be imagined as ‘‘Mexican hats’’ [7, 42, 43]; the study of these 2-dimensional ($n = 1, 2$) and 3-dimensional ($n = 3$) troughs is a classic topic in JT physics [43, 44].

Conversely, for holes in C₆₀⁺ the $h^n \otimes (G + H)$ JT model gives rise to discrete sets of isolated minima [19, 23, 26, 45]. The nature and symmetry of these discrete valleys depends on the details of the e-v couplings and on the interplay with Coulomb interaction. We shall describe here in some detail the minima obtained in this calculation.

To identify these minima, we generate about a hundred randomly distributed distortions away from the I_h high-symmetry point, and let the vibration coordinates relax from there to the closest energy minimum, by combined standard (simplex and conjugate-gradients) minimization algorithms. We then apply the symmetry operations of the icosahedral group to the each minimum found, locating all possible equivalent minima. Although the method

employed is not exhaustive, the application of symmetry and the thoroughness of our search, carried out with a large variety of starting points guarantees in practice the retrieval of all relevant minima. We can readily discard, for example, the few cases where minimization led to saddle points or to secondary, local minima, based on simple comparison of the energy values. In this way, for each n and S , we finally obtain the set of equivalent valleys that are global adiabatic energy minima for C₆₀^{n±}. The amount of ‘‘radial’’ distortion at the adiabatic minima for each mode is tabulated in the Appendix.

In Table 4 we summarize some global properties of the JT energy valleys for C₆₀^{n±} in all spin sectors. In these many-mode JT systems, the local symmetry of an optimal distortion is described in terms of the subgroup $G_{\text{local}} \subset I_h$ of symmetry operations which leave that minimum invariant. The minima in the simple $n = 1$ $S = \frac{1}{2}$ case, where e-e interactions are irrelevant, are believed to be six valleys of D_{5d} symmetry [19, 23, 26] – the alternative possibility of ten D_{3d} valleys apparently disfavored by the specific couplings obtained for fullerene [19]. Table 4 reveals a symmetry between the minima for $n = 4$ $S = 2$ and $n = 1$ $S = \frac{1}{2}$, as well as for $n = 2$ $S = 1$ and $n = 3$ $S = \frac{3}{2}$. These symmetries are at first sight surprising, but can be readily explained by applying a particle-hole transformation to the fermion operators of only one spin kind, in the fully spin-polarized states. This transformation maps the Hamiltonian matrices of an n -particle states (apart from a constant exchange term) into those of $(5 - n)$ particle states, with a sign change of the vibron interaction \hat{H}_{e-v} that shifts each minimum \mathbf{Q}_{min} to the opposite locations $-\mathbf{Q}_{\text{min}}$. We have therefore $V_{4,2}^{\text{ad}}(\mathbf{Q}) = V_{1,1/2}^{\text{ad}}(-\mathbf{Q}) + C$, with $C = -\frac{2}{3}F_2 - \frac{5}{6}F_3 - \frac{5}{6}F_4 = -238$ meV. The same connection between the $n = 2$ $S = 1$ and the $n = 3$ $S = \frac{3}{2}$ adiabatic potentials involves an energy shift $C = -\frac{2}{9}F_2 - \frac{5}{18}F_3 - \frac{5}{18}F_4 = -80$ meV. The same symmetry relates $n = 5$ $S = \frac{5}{2}$ to $n = 0$ $S = 0$, where no JT distortion takes place.

In general, the number of JT valleys (third column of Table 4) is related to the local symmetry. It is basically given by the ratio $|I_h|/|G_{\text{local}}|$ of the order of the icosahedral group (120) to the order of the invariant subgroup G_{local} . However, $n = 5$ holes make an exception to this rule. Here, at half filling, in addition to the I_h symmetry, the system is particle-hole symmetric, i.e. invariant under exchange of creation and annihilation operators of both spin kinds. This transformation leaves the Coulomb Hamiltonian \hat{H}_{e-e} invariant, and again changes sign of the vibronic interaction \hat{H}_{e-v} : hence, given any minimum \mathbf{Q}_{min} , its opposite $-\mathbf{Q}_{\text{min}}$ is also an equivalent minimum of the potential energy surface. For $S = \frac{1}{2}$, this leads to a doubling of the minima: the local C_{2h} symmetry would lead to 30 minima, but 30 additional equivalent minima are added in the opposite positions by particle-hole symmetry. For $S = \frac{3}{2}$ instead, the number of minima remains 30, since for each minimum there is one of the I_h symmetry

² The G_g modes are irrelevant for the negative ions, but relevant for positive ions

Table 3. The three contributions (restoring harmonic potential, e-v coupling, and e-e exchange – the $[Un(n-1)/2]$ term is excluded from \hat{H}_{e-e}) in the adiabatic energy E_{adiab} for $C_{60}^{n\pm}$ in all possible charge and spin states. As usually occurs in JT, the contribution $\langle \hat{H}_{e-v} \rangle = -2 \langle \hat{V}_{\text{vib}} \rangle = -2V_{\text{vib}}(\mathbf{Q}_{\text{min}})$. The following columns report the leading zero-point energy correction E_{zero} [Eq. (15)] and the sum of this correction to the adiabatic energy, representing our best estimate of the energy of each valley, relative to the undistorted state of the ion. For C_{60}^{\pm} , the last column reports the exact energy obtained by Lanczos diagonalization. All energies are in meV. Boldface indicates the ground-state total energy at each n (high spin for cations, low spin for anions). For positive ions, comparison with the exact result in the last column indicates a fairly good approximation already for $n=1$; and we expect the accuracy to be even better for $n=2,3,4,5$ holes.

n	S	$\langle \hat{V}_{\text{vib}} \rangle$	$\langle \hat{H}_{e-v} \rangle$	$\langle \hat{H}_{e-e} \rangle$	E_{adiab}	E_{zero}	$E_{\text{adiab}} + E_{\text{zero}}$	E_{exact}
C_{60}^{m+}								
1	1/2	69	-138	0	-69	-51	-120	-103
2	0	270	-540	141	-129	-72	-201	
	1	99	-197	-43	-142	-92	-234	
3	1/2	267	-534	99	-168	-122	-290	
	3/2	99	-197	-123	-222	-92	-314	
4	0	361	-723	162	-200	-133	-332	
	1	229	-459	19	-211	-134	-345	
	2	69	-138	-238	-308	-51	-359	
5	1/2	308	-616	105	-203	-150	-353	
	3/2	169	-338	-87	-256	-98	-354	
	5/2	0	0	-397	-397	0	-397	
C_{60}^{m-}								
1	1/2	38	-77	0	-38	-113	-152	-76
2	0	149	-298	56	-93	-115	-207	
	1	38	-77	-32	-71	-113	-184	
3	1/2	113	-225	28	-85	-171	-256	
	3/2	0	0	-97	-97	0	-97	

operations, a C_2 rotation, that transforms this minimum into its opposite point³.

Table 4 contains also some information about the connectivity of the minima in \mathbf{Q} space. In many cases, the specification of the number of first, second, etc. neighbors of a given minimum is sufficient to clarify completely the topology of the minima in the 64-dimensional space. In particular, the D_{5d} wells of the $n=1$ $S=\frac{1}{2}$, of the $n=2$ $S=0$, and of the $n=4$ $S=2$ surfaces are located on the six vertexes of five-dimensional regular simplexes, generalizations of the 3D tetrahedron, each minimum being equidistant to all the others. In analogy, the connectivity of the 10 D_{3d} minima for $n=4$ $S=0$ is the same as that depicted in Fig. 1b of Ref. [23] for a different situation. For the other cases of lower symmetry, the number of neighbors of any given order must be complemented by some extra connectivity information, for which we refer to previous work [41]. We only observe that for $n=2$ $S=1$ (equivalently for $n=3$ $S=\frac{3}{2}$), each of the 15 minima is linked to four nearest-neighbor minima, which, in turn, are

linked to more minima, forming a completely connected regular polytope. For $n=3$ $S=\frac{1}{2}$ and $n=4$ $S=1$, the 30 minima are divided into 6 pentagonal “clusters” of five nearest-neighboring minima. In contrast, for $n=5$ $S=\frac{1}{2}$, nearest-neighbor wells come in pairs. Finally, the 30 C_{2h} minima for $n=5$ $S=\frac{3}{2}$, show the largest connectivity, and sit at the vertexes of a highly symmetric polytope.

Figure 1 pictures the electronic state of the holes at the adiabatic valleys of C_{60}^{n+} . As typical of JT, distortions are such that relatively large gaps open between empty and filled levels. For $n > 1$ this single-determinant picture is only approximate: it represents the dominant uncorrelated configuration within the fully correlated exact electronic ground state at each well.

The adiabatic valleys described above are the joint result of e-v couplings and of e-e Coulomb interactions. One can understand better the specific role of Coulomb interaction for the JT distortion by comparing the number and symmetry of the valleys described above to those obtained by the same procedure in a hypothetical noninteracting case, obtained by setting all $F_j = 0$. Doing that, we find basically the same general picture of valleys for $n=1$ (obviously), but also for $n=2$, $n=3$, $n=4$ $S=1, 2$ and $n=5$ $S=\frac{3}{2}, \frac{5}{2}$. In all remaining cases the e-e correlations

³ The real-space inversion, acting on the real-space displacements, leaves all JT-active normal-mode coordinates invariant, since they are even (g) under inversion.

Table 4. Number and local symmetry of the JT minimal valleys for each charge n and spin S in $C_{60}^{n\pm}$ ions. The 5th column gives, for each given valley, the number of equivalent valleys that are first, second, etc. neighbors of that valley in \mathbf{Q} space. The last column gives the total magnitude of the dimensionless JT distortion at each minimum.

n	S	number of minima	local symmetry	number of 1 st , 2 nd , 3 rd , 4 th ... neighbor minima	distortion $ \mathbf{Q}_{\min} $
C_{60}^{m+}					
1	1/2	6	D_{5d}	5	1.58
2	0	6	D_{5d}	5	3.12
	1	15	D_{2h}	4 4 4 2	1.87
3	1/2	30	C_{2h}	2 1 2 4 4 2 2 2 2 4 4 2	3.08
	3/2	15	D_{2h}	4 4 4 2	1.87
4	0	10	D_{3d}	3 6	3.52
	1	30	C_{2h}	2 2 2 2 1 4 4 4 6 2	2.85
	2	6	D_{5d}	5	1.58
5	1/2	60	C_{2h}	1 2 2 4 4 4 2 2 2 4 2 2 4 2 2 4 2 2 4 4 4 2 2 1 1	3.27
	3/2	30	C_{2h}	8 12 8 1	2.46
	5/2	1	I_h	0	0
C_{60}^{m-}					
1	1/2	∞	C_i or higher	∞	0.91
2	0	∞	C_i or higher	∞	1.79
	1	∞	C_i or higher	∞	0.91
3	1/2	∞	C_i or higher	∞	1.55
	3/2	1	I_h	0	0

also introduces a qualitative change in the topology and local symmetry of the minima. Without interactions, 15 D_{2h} minima would replace the 10 D_{3d} minima for $n = 4$ $S = 0$; and 20 D_{3d} minima replace the 60 C_{2h} minima for $n = 5$ $S = 1/2$. In all cases (except of course $n = 1$ and the symmetric $n = 4$ $S = 2$), the amount of distortion is a few per cent larger in the uncorrelated case than when exchange is included, as expected from competing interactions. For example, without correlation, the total distortion for $n = 2$ $S = 0$ would be 3.16, i.e. exactly twice the distortion for $n = 1$, as routinely occurs in JT when exchange plays no role.

4 Zero-point quantum corrections

The vibrational quantum kinetic energy, a quantity neglected at the adiabatic level, does in fact contribute quite substantially to the JT energetics of these multi-mode systems characterized by intermediate couplings. The zero-point energy gain associated to the softening of the vibrational frequency at the JT-distorted minima is illustrated in Fig. 2. It represents the leading quantum correction to the static JT energetics [22,41,46]. To compute this correction for each charge n and spin S , by finite differences we evaluate the Hessian matrix of the second-order derivatives of the lowest adiabatic potential sheet, at each of the

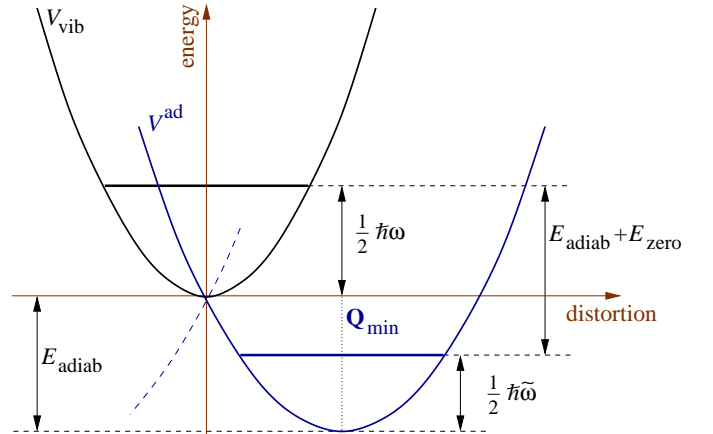


Fig. 2. A pictorial illustrating the origin of the zero-point energy gain due to vibrational softening at the JT well. The horizontal axis represents a generic distortion coordinate, the horizontal thick lines represent the quantum ground states in the non-JT and JT potential wells.

adiabatic JT minima:

$$\mathcal{H}(n, S)_{\alpha\alpha'} = \left. \frac{\partial^2 V_{n,S}^{\text{ad}}(\mathbf{Q})}{\partial Q_\alpha \partial Q_{\alpha'}} \right|_{\mathbf{Q}_{\min}(n,S)} \quad (13)$$

where α is a collective index for $\{i \Lambda \mu\}$. The normal-mode frequencies $\tilde{\omega}_j$ in each well are computed by taking the

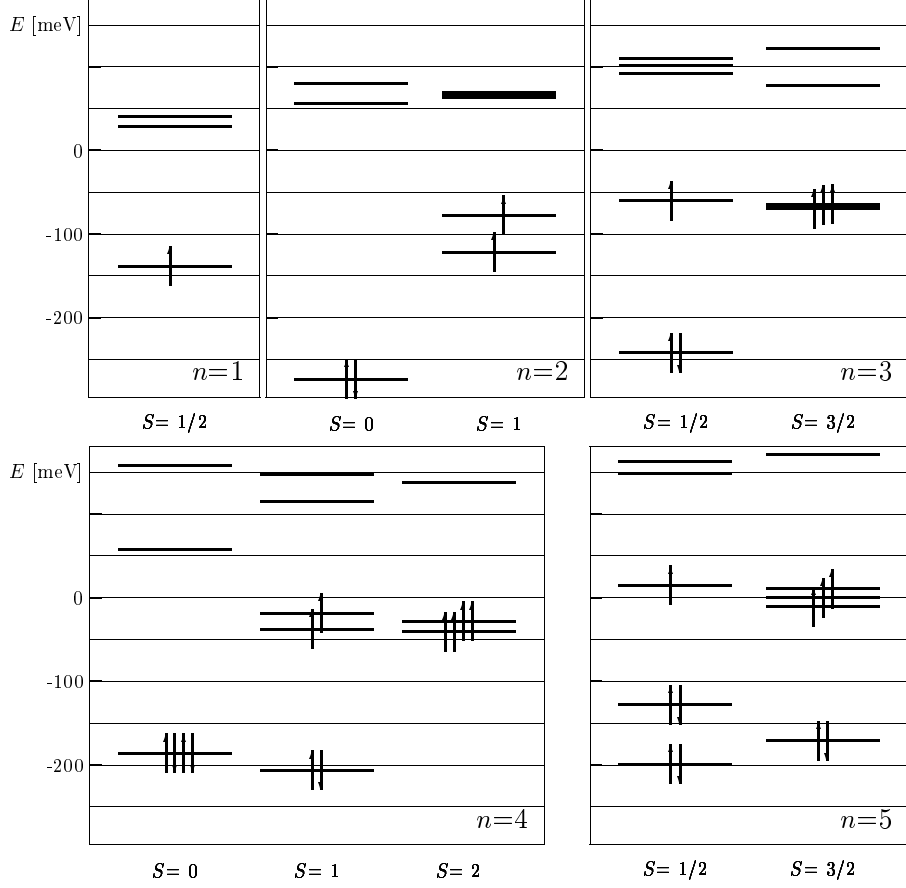


Fig. 1. A line-spectrum representation of the dominant single-determinant electronic state in the optimal adiabatic configuration of C_{60}^{n+} for each spin S . Levels are ordered for holes.

square roots of the eigenvalues of the dynamical matrix defined by

$$\mathcal{D}(n, S)_{\alpha\alpha'} = \delta_{\alpha\alpha'} \omega_{\alpha}^2 + \omega_{\alpha}^{1/2} [\mathcal{H}(n, S)_{\alpha\alpha'} - \delta_{\alpha\alpha'} \omega_{\alpha}] \omega_{\alpha'}^{1/2}. \quad (14)$$

The $-\delta_{\alpha\alpha'} \omega_{\alpha}$ term removes the restoring term from \hat{V}_{vib} in $V_{n,S}^{\text{ad}}$, and the $\omega_{\alpha}^{1/2}$ are introduced by the standard change of variables to correct for the different “mass” coefficients of different coordinates Q_{α} in \hat{T}_{vib} . By retaining the harmonic expansion of the adiabatic potential around a minimum the quantum ground state energy of this potential well is estimated at $\sum_j \frac{1}{2} \hbar \tilde{\omega}_j$ above the classical minimum, due to zero-point motion. As illustrated in Fig. 2, the difference between this and the original zero-point energy $\sum_{\alpha} \frac{1}{2} \hbar \omega_{\alpha}$ at the neutral-molecule harmonic minimum provides the leading quantum correction

$$E_{\text{zero}}(n, S) = \frac{1}{2} \left[\sum_j \hbar \tilde{\omega}_j(n, S) - \sum_{i\Lambda\mu} \hbar \omega_{i\Lambda} \right], \quad (15)$$

to the “classical” valley energy E_{adiab} . $E_{\text{zero}}(n, S)$ in JT problems is systematically found to be negative in sign, corresponding to softer vibrations, and a shallower valley bottom at the new minima than for the $n = 0$ non-JT

molecule. Table 3 reports the zero-point correction computed as described above, and the estimate of the ground-state energy obtained by adding the correction E_{zero} to E_{adiab} .

For C_{60}^{n-} , the zero-point corrections favor low-spin states for both $n = 2$ (already a $S = 0$ ground state at the adiabatic level) and $n = 3$, where the zero-point correction only affects $S = 1/2$, lowering it well below the uncorrected $S = 3/2$. Note however that in the $t^n \otimes H$ JT for the anions, the two ($n = 1$ and 2) and three ($n = 3$) “soft” modes along the trough are associated to vanishing frequencies $\tilde{\omega}_j$. They formally contribute a vanishing zero-point energy to the first sum of Eq. (15). In our calculation this produces unreasonably large (negative) zero-point corrections, larger even than the adiabatic energies. These null terms are correct only in the limit of infinite coupling, where the “size” of the flat trough is infinite, and indeed the free pseudorotational motion carries no zero-point energy. For C_{60}^{n-} , where coupling is finite, and not especially large, the trough has a finite size of order g^2 , which provides some amount of quantum confinement, associated to a zero-point kinetic energy of order g^{-2} , as was described in Ref. [7,43]. These extra “confinement” corrections should be especially sizable when the vibrational wavefunctions have the nontrivial nodal structure due to

the boundary conditions associated to an electronic Berry phase, i.e. for $n = 1$, $n = 2$ $S = 1$, and $n = 3$ $S = 1/2$ [7], but should not change the conclusion that all C_{60}^{n-} ions should favor low spin.

To get an estimate of the validity of the approximations employed here, we can compare with the ground state energy of C_{60}^- obtained by means of an essentially exact calculation (a Lanczos diagonalization on a truncated, but well converged, basis) of our Hamiltonian (1) with the same parameters. The exact energy gain obtained is -76 meV, which falls in between the adiabatic (-38 meV) and zero-point corrected (-152 meV) values. Not surprisingly, in this rather weakly coupled case, the zero-point correction largely overshoots the correct value. As charges $n > 1$ are associated to larger distortions, thus effectively to stronger couplings, we expect that the zero-point corrected energy should be of better quality there. However, the relative size of the zero-point and confinement corrections to the adiabatic energy makes the whole strong-coupling expansion rather questionable for all the anions. Thus the C_{60}^{n-} results as reported here serve mostly for comparison with those of the cations. For cations we expect in fact the quality of our zero-point corrected results to be substantially better.

In the C_{60}^{n+} ions too, in fact, the zero-point energy corrections are rather large, but here the magnitude of the adiabatic energy gains is even larger. The difference with the anions is due both to the larger couplings and to the structure of localized minima as opposed to a flat trough. Comparison of Table 3 and Table 4 shows that situations with a larger number of minima generally yield larger values of the correction $|E_{\text{zero}}|$. Quantum kinetic energy in this respect behaves a bit like statistical entropy, in that it favors numerous shallower minima against few deeper ones. The zero-point correction peaks at ≈ -150 meV for $n = 5$ $S = \frac{1}{2}$, where the minima are shallow and the lowest vibrational frequency is as small as $\tilde{\omega}_1 \approx 10$ meV in this case. On the contrary, few well spaced minima, as for $n = 1$ $S = 1/2$ and $n = 2$ $S = 0$ are associated to a smaller zero-point gain of the order ≈ -100 meV. In the close competition between Coulomb physics (Hund's rules) and JT physics (anti-Hund behavior), the zero-point correction is not irrelevant. As shown by the last column of Table 3, it reduces drastically the large adiabatic spin gap between the high-spin ground state and the lowest spin excitations for $n = 4$ and for $n = 5$. Remarkably, the zero-point correction favors the high-spin state instead in C_{60}^{2+} : the excitation energy to $S = 0$ is enhanced by the quantum correction from 13 meV to 33 meV. Thus although the estimated spin gap is not especially large nor especially reliable, this circumstance makes in our view the prediction of a $S = 1$ magnetic C_{60}^{2+} ion stronger than for the other cations.

Could we go beyond the zero point correction, and get more accurate results? Not easily at this stage. The zero-point correction represents the g^0 term of a large-coupling expansion, where the adiabatic energy E_{adiab} is the leading (g^2) term. The next corrections to be considered, of order g^{-2} and higher, are associated with anharmonicity

of the valleys and tunneling amongst them (in the holes case), and also to mixing of the upper adiabatic potential surfaces with the associated geometric-phase effects [7, 23, 47, 48]. A full quantitative description of these effects would imply a much more sophisticated treatment of the quantum problem than the simple semiclassical expansion applied here, and that is beyond the scope of the present paper. To get an estimate of the importance of these higher-order corrections, we can again compare, now for C_{60}^+ the adiabatic (-69 meV) and the zero-point corrected (-120 meV) ground-state energy gains to the exact one, obtained by a well converged Lanczos diagonalization, which is -103 meV. We see that although E_{zero} still overshoots the quantum corrections the adiabatic gain, the residual error of 17 meV is now fairly small. The accuracy expected for the zero-point corrected energy gains for all other cations $C_{60}^{n+>1+}$ is even better. In fact, the distortions there are larger, tunneling is suppressed, and the approximation of isolated harmonic JT valleys should be much better than for $n = 1$. Thus, even if a check with the Lanczos method would be too cumbersome here because of the excessive basis size required for $n > 1$, our zero-point corrected results of Table 3 should be regarded as practically exact, for the assumed coupling parameters.

5 Discussion and Conclusions

The main output of this paper is a determination of the ground state spin, energy, and distortion magnitude of JT distorted C_{60}^{n+} molecular ions.

Calculations include both e-e and e-v interactions as derived from earlier first-principles calculations, as well as very important quantum vibrational effects, due to the small mass of the carbon nuclei. The latter are taken into account approximately by including the changes of vibrational zero-point energy from the undistorted to the different distorted states. These zero-point corrections are shown to be generally large. In C_{60}^{3-} they are even capable of turning a high-spin ground state into a low-spin one. As the coupling and thus the distortions are fairly large, quadratic and higher-order (in \mathbf{Q}) e-v interactions and vibration anharmonicity could also be relevant. The present calculation was however carried out strictly in the linear e-v coupling approximation.

The parameters used in this calculation, both for e-e and e-v interaction could be somewhat underestimated by the local density approximation used in their determination, as discussed in Ref. [5, 19]. Consequently, both the Coulomb repulsion and the JT effective e-e attraction calculated within the local density approximation might need some correcting in their absolute values. The balance between these two opposing interactions is delicate in C_{60}^{n-} ions (as demonstrated by the presence of both high-spin and low-spin local ground states in different chemical environments [9, 15, 49, 50, 51, 52, 53]), but low-spin ground states are generally believed to prevail, in accord with the present calculation. Contrary to that, in C_{60}^{n+} , Hund-rule magnetism and high-spin ground states are predicted to dominate. Experimentally, so far we found no evidence

concerning gas phase C_{60}^{n+} ions that we could usefully address. We do not know at this moment whether the lifetime of positive ions against fragmentation would permit experiments to be conducted, and if so whether the ground-state spins and JT distortions could be determined and compared with our predictions. Singly charged C_{60}^+ ions have been created in solution [54], in molecular-beam photoemission [16,17], and in storage rings [55]: but they are irrelevant to our present question.

More encouragingly, higher positive charge states have been pursued in solid-state acceptor compounds [56,57]. The interplay of intra-molecular physics with electron hopping in a hypothetical fullerene-cation based solid-state conducting compound is very interesting. Our results suggest that magnetism should be important in these compounds, at least so long as the hole bands remain relatively narrow. The HOMO bands of the proposed acceptor compounds $(AsF_6)_2C_{60}$ and $(SbF_6)_2C_{60}$ can indeed be expected to be rather narrow. In $(AsF_6)_2C_{60}$, based on a bct unit cell with lattice parameters $a = b = 12.8 \text{ \AA}$, $c = 12.4 \text{ \AA}$, we can extract a fullerene-fullerene inter-center distance 10.97 \AA , significantly larger than 10.02 \AA of pure C_{60} . On the other hand, the on-site Hubbard U estimated for holes is comparable to or slightly larger than that for electrons. It seems reasonable therefore to surmise that hole-doped $(AsF_6)_2C_{60}$ could be, like the electron-doped $K_3NH_3C_{60}$ [58], as well as A_4C_{60} [59,60], a Mott-JT insulator. Unlike the electron-doped compounds, where the JT distorted C_{60}^{n-} molecular ion was in a low-spin configuration ($S = 1/2$ for $n = 3$, $S = 0$ for $n = 2, 4$), we expect in the divalent acceptor fullerene compound that the positive C_{60}^{2+} ions should be in a high-spin, $S = 1$ JT-distorted state. If so, they would constitute an exciting example of molecular Hund’s rule magnetism. The magnetic coupling between neighboring C_{60}^{2+} $S = 1$ ions in these compounds should most likely be weak and antiferromagnetic [61]. It might be interesting to pursue this and to seek a Néel state of some kind at very low temperatures. Pressure studies of the electron-doped compounds have revealed insulator-metal transitions such as that of Rb_4C_{60} [62], and also insulator-superconductor transitions such as that of $K_3NH_3C_{60}$ [63]. Pressure studies of fullerene acceptors could be an interesting line to pursue in the future. More generally, the realization of a well characterized fullerene hole conductor remains a worthy challenge for the future.

Acknowledgments

We are indebted to M. Wierzbowska, G. Santoro, G. Onida, and L. Reatto for useful discussions. This work was supported by the European Union, contracts ERBFMRXCT-970155 (TMR FULPROP), covering in particular the post-doctoral work of M. Lüders; by HPRI-CT-1999-00048 (MINOS) and the CINECA Casalecchio Supercomputing Center for computing time and for a fellowship; and by MIUR COFIN01, and FIRB RBAU017S8R of MIUR.

Table 5. The dimensionless JT distortions $|\hat{Q}_{iA}|$ at the minima of C_{60}^{n-} , for each H_g mode and allowed spin S .

n	S	dimensionless distortions of H_g modes								
1	1/2	0.412	0.489	0.350	0.224	0.193	0.138	0.315	0.289	
2	0	0.813	0.965	0.691	0.442	0.381	0.273	0.622	0.571	
2	1	0.412	0.489	0.350	0.224	0.193	0.138	0.315	0.289	
3	1/2	0.706	0.838	0.600	0.384	0.331	0.237	0.540	0.496	
3	3/2	0.000	0.000	0.000	0.000	0.000	0.000	0.000	0.000	

A Appendix

Tables 5 and 6 report the individual amount of JT distortion associated to each normal mode of C_{60} at any equivalent adiabatic minimum of $C_{60}^{n\pm}$, for all spin- S sectors. The distortions are given in the dimensionless units of the coordinate operators $|\hat{Q}_{iA}|$. The appropriate length scales $x_0(\omega_{iA}) = \sqrt{\hbar/(\omega_{iA} m_C)}$ for the G_g and H_g modes of C_{60} are: 76.3, 70.4, 60.3, 50.3, 46.1, 43.0, and 103.7, 80.9, 62.6, 59.8, 50.1, 47.0, 43.9, 42.1 pm, respectively. For C_{60}^{n-} the amount of “radial” distortion is independent of the point chosen along the trough. As expected, the modes characterized by the strongest coupling show the largest distortion. The mode associated to the largest distortion is therefore the lowest H_g mode (see Table 1) in the cations. Note also that the G_g modes do not contribute to the distortions of D_5 symmetry, but contribute to all the lower-symmetry minima.

References

1. T. L. Makarova, B. Sundqvist, R. Höhne, P. Esquinazi, Y. Kopelevich, P. Scharff, V. A. Davydov, L. S. Kashevarova, and A. V. Rakhmanina, *Nature (London)* **413**, 716 (2001).
2. R. A. Wood, M. H. Lewis, M. R. Lees, S. M. Bennington, M. G. Cain, and N. Kitamura, *J. Phys.: Condens. Matter* **14**, L385 (2002).
3. R. L. Martin and J. P. Ritchie, *Phys. Rev. B* **48**, 4845 (1993).
4. J. E. Han and O. Gunnarsson, *Physica B* **292**, 196 (2000).
5. M. Lüders, A. Bordoni, N. Manini, A. Dal Corso, M. Fabrizio, and E. Tosatti, *Philos. Mag. B* **82**, 1611 (2002).
6. L. Bergomi and T. Jolicœur, *Comptes Rendus Acad. Sci. II* **318**, 283 (1994).
7. A. Auerbach, N. Manini, and E. Tosatti, *Phys. Rev. B* **49**, 12998 (1994).
8. N. Manini, E. Tosatti, and A. Auerbach, *Phys. Rev. B* **49**, 13008 (1994).
9. V. Brouet, H. Alloul, T. N. Le, S. Garaj, and L. Forro, *Phys. Rev. Lett.* **86**, 4680 (2001).
10. A. Rajca, S. Utamapanya, and D. J. Smithhisler, *J. Org. Chem.* **58**, 5650, (1993).
11. A. Rajca, S. Rajca, and J. Wongsriratanakul, *Chem. Commun.* **2000**, 1021 (2000).
12. V. Brouet, H. Alloul, F. Quere, G. Baumgartner, and L. Forro, *Phys. Rev. Lett.* **82**, 2131 (1999).
13. P. M. Allemand, K. C. Kemani, A. Koch, F. Wudl, K. Holzer, S. Donovan, G. Grüner, and J. D. Thompson,

Table 6. The dimensionless JT distortions $|\hat{Q}_{iA}|$ at the minima of C_{60}^{n+} , for each G_g and H_g mode and each allowed spin S .

n	S	Symmetry	distortions of G_g modes						distortions of H_g modes							
1	0	D_{5d}	0.000	0.000	0.000	0.000	0.000	0.000	1.36	0.473	.00459	0.35	0.023	0.205	0.379	0.333
2	0	D_{5d}	0.000	0.000	0.000	0.000	0.000	0.000	2.69	0.935	.0095	0.692	.0455	0.405	0.749	0.657
2	1	D_{2h}	.0755	.0102	.0799	.0623	.0227	.0466	1.58	0.611	0.138	0.404	.0516	0.262	0.486	0.346
3	1/2	C_{2h}	.0548	.0074	.0580	.0452	.0165	.0339	2.62	1.01	0.185	0.669	.0799	0.433	0.801	0.571
3	3/2	D_{2h}	.0755	.0102	.0799	.0623	.0227	.0466	1.58	0.611	0.138	0.404	.0516	0.262	0.486	0.346
4	0	D_{3d}	.0828	.0112	.0877	.0683	.0249	.0512	2.88	1.30	0.494	0.728	0.153	0.553	1.02	0.486
4	1	C_{2h}	0.074	0.010	.0782	0.061	.0223	.0457	2.39	0.968	0.228	0.609	.0879	0.414	0.767	0.486
4	2	D_{5d}	0.000	0.000	0.000	0.000	0.000	0.000	1.36	0.473	.0046	0.35	0.023	0.205	0.379	0.333
5	1/2	C_{2h}	0.101	.0135	0.106	.0827	.0302	.0619	2.70	1.17	0.401	0.683	0.129	0.500	0.926	0.492
5	3/2	C_{2h}	.0384	.0053	.0411	0.032	.0117	0.024	2.12	0.756	.0391	0.544	.0427	0.327	0.605	0.503
5	5/2	I_h	0.000	0.000	0.000	0.000	0.000	0.000	0.00	0.000	0.000	0.000	0.000	0.000	0.000	0.000

- Science **253**, 301 (1991); K. Tanaka, A. A. Zakhidov, K. Yoshizawa, K. Okahara, T. Yamabe, K. Yakushi, K. Kikuchi, S. Suzuki, I. Ikemoto, and Y. Achiba, Phys. Lett. A **164**, 221 (1992).
14. B. Narymbetov, A. Omerzu, V. V. Kabanov, M. Tokumoto, H. Kobayashi, and D. Mihailovic, Nature (London) **407**, 883 (2000); B. Narymbetov, A. Omerzu, V. V. Kabanov, M. Tokumoto, H. Kobayashi, and D. Mihailovic, Phys. Solid State **44**, 437 (2002).
15. D. P. Arovas and A. Auerbach, Phys. Rev. B **52**, 10114 (1995).
16. P. Brühwiler, A. J. Maxwell, P. Balzer, S. Andersson, D. Arvanitis, L. Karlsson, and N. Mårtensson, Chem. Phys. Lett. **279**, 85 (1997).
17. S. E. Canton, A. J. Yench, E. Kuk, J. D. Bozek, M. C. A. Lopes, G. Snell, and N. Berrah, Phys. Rev. Lett. **89**, 045502 (2002).
18. A. M. Panich, P. K. Ummat, and W. R. Datars, Solid State Commun. **121**, 367 (2002).
19. N. Manini, A. Dal Corso, M. Fabrizio, and E. Tosatti, Philos. Mag. B **81**, 793 (2001).
20. M. Fabrizio and E. Tosatti, Phys. Rev. B **55**, 13465 (1997).
21. W. R. Datars, J. D. Palidwar, and P. K. Ummat, J. Phys. Chem. Solids **57**, 977 (1996).
22. N. Manini and E. Tosatti, Phys. Rev. B **58**, 782 (1998).
23. N. Manini and P. De Los Rios, Phys. Rev. B **62**, 29 (2000).
24. P. H. Butler, *Point Group Symmetry Applications* (Plenum, New York, 1981).
25. E. Tosatti, N. Manini, and O. Gunnarsson, Phys. Rev. B **54**, 17184 (1996).
26. A. Ceulemans, and P. W. Fowler, J. Chem. Phys. **93**, 1221 (1990).
27. M. Saito, Phys. Rev. B **65**, 220508 (2002).
28. R. D. Bendale, J. F. Stanton, and M. C. Zerner, Chem. Phys. Lett., **194**, 467 (1992).
29. M. Wierzbowska, M. Lüders, and E. Tosatti, unpublished.
30. N. Manini, P. Gattari, and E. Tosatti (unpublished), and P. Gattari, <http://www.mi.infn.it/manini/theses/gattari.pdf>.
31. C. M. Varma, J. Zaanen, and K. Raghavachari, Science **254**, 989 (1991).
32. M. Schlüter, M. Lannoo, M. Needels, G. A. Baraff, and D. Tománek, Phys. Rev. Lett. **68**, 526 (1991); J. Phys. Chem. Solids **53**, 1473 (1992).
33. V. P. Antropov, O. Gunnarsson, and A. I. Lichtenstein, Phys. Rev. B **48**, 7651 (1993).
34. W. H. Green Jr., S. M. Gorun, G. Fitzgerald, P. W. Fowler, A. Ceulemans, and B. C. Titeca, J. Phys. Chem. **100** 14892 (1996).
35. O. Gunnarsson, H. Handschuh, P. S. Bechthold, B. Kessler, G. Ganteför, and W. Eberhardt, Phys. Rev. Lett. **74**, 1875 (1995); O. Gunnarsson, Phys. Rev. B **51**, 3493 (1995).
36. R. D. Cowan, *The Theory of Atomic Structure and Spectra* (Univ. of California Press, Berkeley-CA, 1981).
37. A. V. Nikolaev and K. H. Michel, J. Chem. Phys. **117**, 4761 (2002).
38. N. Manini and E. Tosatti, in *Recent Advances in the Chemistry and Physics of Fullerenes and Related Materials: Volume 2*, edited by K. M. Kadish and R. S. Ruoff (The Electrochemical Society, Pennington, NJ, 1995), p. 1017.
39. P. De Los Rios, N. Manini, and E. Tosatti, Phys. Rev. B **54**, 7157 (1996).
40. C. P. Moate, J. L. Dunn, C. A. Bates, and Y. M. Liu, J. Phys.: Condens. Matter **9**, 6049 (1997).
41. M. Lüders and N. Manini, cond-mat/0211375 - to be published in *Advances in Quantum Chemistry* (2003), as Proceedings of the XVI Jahn-Teller Conference - Catholic University of Leuven-Belgium, 2002.
42. M. C. M. O'Brien, J. Phys. C **5**, 2045 (1972).
43. M. C. M. O'Brien, Phys. Rev. B **53**, 3775 (1996).
44. C. C. Chancey and M. C. M. O'Brien, *The Jahn-Teller Effect in C_{60} and Other Icosahedral Complexes* (Princeton Univ. Press, Princeton, 1997).
45. C. P. Moate, M. C. M. O'Brien, J. L. Dunn, C. A. Bates, Y. M. Liu, and V. Z. Polinger, Phys. Rev. Lett. **77**, 4362 (1996).
46. The treatment of zero-point corrections in Ref. [41] is incorrect. The present version gives the corrected formulas and values.
47. N. Manini and P. De Los Rios, J. Phys.: Condens. Matter **10**, 8485 (1998).
48. M. Baer, Phys. Rep. **358**, 75 (2002).

49. R. F. Kieff, T. L. Duty, J. W. Schneider, A. MacFarlane, K. Chow, J. W. Elzey, P. Mendels, G. D. Morris, J. H. Brewer, E. J. Ansaldo, C. Niedermayer, D. R. Noakes, C. E. Stronach, B. Hitti, and J. E. Fischer, *Phys. Rev. Lett.* **69**, 2005 (1992).
50. G. Zimmer, M. Mehring, C. Goze, and F. Rachdi, in *Physics and Chemistry of Fullerenes and Derivatives*, edited by H. Kuzmany, J. Fink, M. Mehring, and S. Roth (World Scientific, Singapore, 1995), p. 452.
51. I. Lukyanchuk, N. Kirova, F. Rachdi, C. Goze, P. Molinie, and M. Mehring, *Phys. Rev. B* **51**, 3978 (1995).
52. K. Prassides, S. Margadonna, D. Arcon, A. Lappas, H. Shimoda, and Y. Iwasa, *J. Am. Chem. Soc.* **121**, 11227 (1999).
53. A. Schilder, H. Klos, I. Rystau, W. Schütz, and B. Gotschy, *Phys. Rev. Lett.* **73**, 1299 (1994).
54. C. A. Reed, K.-C. Kim, R. D. Bolskar, and L. J. Mueller, *Science* **289**, 201 (2000).
55. S. Tomita, J. U. Andersen, C. Gottrup, P. Hvelplund, and U. V. Pedersen, *Phys. Rev. Lett.* **87**, 073401 (2001).
56. W. R. Datars and P. K. Ummat, *Solid State Commun.* **94**, 649 (1995).
57. A. M. Panich, H.-M. Vieth, P. K. Ummat, and W. R. Datars, *Physica B* **327**, 102 (2003).
58. N. Manini, G. E. Santoro, A. Dal Corso, and E. Tosatti, *Phys. Rev. B* **66**, 115107 (2002).
59. M. Capone, M. Fabrizio, and E. Tosatti, *Phys. Rev. Lett.* **86**, 5361 (2001).
60. M. Capone, M. Fabrizio, C. Castellani, and E. Tosatti, *Science* **296**, 2364 (2002).
61. C. A. Reed and R. D. Bolskar, *Chem. Rev.* **100**, 1075 (2000).
62. R. Kerkoud, P. Auban-Senzier, D. Jerome, S. Brazovskii, I. Luk'yanchuk, N. Kirova, F. Rachdi, and C. Goze, *J. Phys. Chem. Solids* **57**, 143 (1996).
63. S. Margadonna, K. Prassides, H. Simoda, Y. Iwasa, and M. Mézouar, *Europhys. Lett.* **56**, 61 (2001).